NLO corrections to the *B*-hadron energy distribution of heavy charged Higgs boson decay in the general-mass-variable-flavor-number scheme

P. Sartipi Yarahmadi[1] and S. Mohammad Moosavi Nejad[1,2,*]

[1]*Department of Physics, Yazd University, P.O. Box 89195-741, Yazd, Iran*
[2]*School of Particles and Accelerators, Institute for Research in Fundamental Sciences (IPM), P.O. Box 19395-5531, Tehran, Iran*

(Received 19 July 2022; accepted 29 August 2022; published 27 September 2022)

Since there is no fundamental charged scalar boson in the Standard Model (SM) of particle physics then the discovery of each charged scalar boson would clearly represent an instant evidence of physics beyond the SM. In this regard, searching for charged Higgs bosons is unique and have been the center of attention of colliders such as the CERN LHC. In the present work, we study a proposed channel to search for heavy charged Higgses at the current and future colliders. In this channel we study the scaled-energy distribution of bottom-flavored mesons (B) inclusively produced in heavy charged Higgs decay, i.e., $H^+ \to t\bar{b} \to B + X$. This study is performed within the framework of two Higgs doublet model using the general-mass variable-flavor-number scheme where the b-quark mass is preserved from the beginning. Our results will be compared with the ones calculated in the zero-mass variable-flavor-number scheme where the zero mass approximation is adopted for the bottom quark. We find that most reliable predictions can be achieved through the massive scheme.

DOI: 10.1103/PhysRevD.106.055040

I. INTRODUCTION

The recent measurement of the W-boson mass reported by CDF-II Collaboration [1] is significantly heavier than that of the SM prediction; 7σ standard deviations away from the SM prediction. In order to explain this anomaly the addition of extra fields seems inevitable; therefore, it could be a window towards new physics beyond the SM. Various models beyond the SM such as two Higgs doublet model (2HDM) have been employed so far to interpret this anomaly. These new models have basically been created to solve many remaining open questions in the SM. In many extensions of the SM such as the 2HDMs [2] (minimal extensions of the SM) the Higgs sector of model is typically extended by adding an extra doublet of complex Higgs fields. In the 2HDM, after spontaneous symmetry breaking two scalar Higgs doublets (H_1 and H_2) yield three physical neutral Higgs bosons (h, H, A) and a pair of charged Higgs bosons $H^{\pm}$ [3]. The lightest CP-even Higgs boson h can align with the properties of SM. Note that, in the 2HDMs after imposing a discrete symmetry which gives natural flavor conservation the 2HDMs can be classified into four categories—Type I, II, III, and IV—according to the couplings of doublets to the fermions. The minimal supersymmetric standard model (MSSM) [4] is one of the most popular and very well-studied scenarios in the theories beyond the SM where one doublet couples to up quarks and the other to down quarks and charged leptons. It predicts rich and various phenomenology which is testable in colliders, and also its Higgs sector is a Type-II 2HDM which provides elegant solutions to some of the short comings of the SM.

Since, there is no fundamental charged scalar boson in the SM then the discovery of each charged scalar boson shows an instant evidence of physics beyond the SM. Charged scalar Higgs bosons could be lighter or heavier than the top quark. Although, the results of the CMS [5] and ATLAS [6] Collaborations at the CERN large hadron collider (LHC) have excluded a large region in the MSSM $m_{H^{\pm}} - \tan\beta$ parameter space for $m_{H^{\pm}} = 80$–160 GeV corresponding to the entire range of $\tan\beta$ up to 60. Here, $\tan\beta$ shows the ratio of vacuum expectation values of the neutral components of the two Higgs doublets. This exclusion means that there is no much chance to find light charged Higgs bosons ($m_{H^{\pm}} \leq m_t$) in the MSSM framework and all efforts should concentrate on probing the heavy ones, i.e., $m_{H^{\pm}} > m_t$. It should be noted that, a general 2HDM framework with flavor-changing neutral currents (FCNCs) controlled under some structures in the Yukawa matrices can still allow a light charged Higgs, see Refs. [7–9]. Very recent experimental results confirm a light charged Higgs boson with a mass of around 130 GeV [10].

In many models, a heavy charged Higgs boson is predicted to decay predominantly either to a tau and its associated neutrino or to a top and a bottom quark

*mmoosavi@yazd.ac.ir

($H^+ \to t\bar{b}$) where the top quark itself decays to W^+ boson. Also, the created bottom quark finally hadronizes to produce observable hadrons such as, in the most probable case, bottom-flavored hadrons B. At colliders, B-hadrons could be identified by a displaced decay vertex associated with charged lepton tracks. The decay channel $H^+ \to t\bar{b}$ have been studied by the ATLAS and CMS Collaborations in proton-proton collisions at the center-of-mass energies of 8 [11] and 13 TeV [12–14] so a small excluded region in the MSSM $m_{H^\pm} - \tan\beta$ parameter space has been reported. In other words, large regions in the parameter space are still allowed and corresponding searches are in progress.

In our previous work [15], using the scenario of 2HDM we have studied the energy spectrum of bottom-flavored mesons B inclusively produced in the decay of charged Higgs bosons, i.e., $H^+ \to t\bar{b}(\to B + \text{jets})$. For this study, we simply worked in the massless scheme or zero-mass variable-flavor-number (ZM-VFN) scheme where the mass of the b-quark is set to zero from the beginning. There has been shown that in the limit of vanishing bottom quark mass the results in all classes of 2HDM scenario are the same. In the present work, using the general-mass variable-flavor-number (GM-VFN) scheme where the b-quark mass is preserved ($m_b \neq 0$) we will improve our previous results and show that the effect of b-quark mass is not ignorable for all values of $m_{H^\pm}$ and $\tan\beta$ and leads to very different model-dependent results for the energy spectrum of B-mesons. To describe the b-quark hadronization process ($b \to B + \text{jets}$) we apply the nonperturbative fragmentation functions that are obtained through a global fit to e^-e^+ data from CERN LEP1 and SLAC SLC, exploiting their universality and scaling violations.

This paper is organized as follows. In Sec. II we briefly describe the scenario of 2HDM and present the parton-level expressions for the next-to-leading order (NLO) QCD corrections to the tree-level rate of $H^+ \to t\bar{b}$ in the fixed-flavor-number scheme (FFNs). In Sec. III the GM-VFN scheme is described by introducing the nonperturbative fragmentation functions $(b, g) \to b$. In Sec. III our hadron-level results will be presented by working in the GM-VFN scheme. In Sec. IV our conclusions are summarized.

II. PARTON LEVEL RESULTS FOR $H^+ \to t\bar{b}$

A. Born-level rate

In order to obtain the energy spectrum of B-hadrons inclusively produced in heavy charged Higgs decay, i.e., $H^+ \to t\bar{b} \to B + X$, we first need to have the QCD radiative corrections to the differential partial decay width of the process $H^+ \to \bar{b}t$, i.e., $d\tilde{\Gamma}_i(H^+ \to t\bar{b}(+g))/dx_i (i = b, g)$ where x_i stands for the scaled-energy of b-quarks or gluons. Radiation of real gluon occurs at NLO approximation. For this purpose we work in the 2HDM (Types I and II with natural flavor conservation) where the vacuum expectation values of the doublets H_1 and H_2 give masses to the down-type and up-type quarks, respectively. The vacuum expectation values of H_1 and H_2, i.e., $\mathbf{v}_1$ and $\mathbf{v}_2$, are related to the Fermi constant as $\mathbf{v}_1^2 + \mathbf{v}_2^2 = (\sqrt{2}G_F)^{-1}$ and their ratio is a free parameter which is parametrized as $\tan\beta = \mathbf{v}_2/\mathbf{v}_1$. A relevant linear combination of the charged components of H_1 and H_2 also creates the physical charged Higgs H^+: $H^+ = \cos\beta H_2^+ - \sin\beta H_1^+$.

It should be noted that, in a general model with two Higgs doublets, the generic Higgs coupling to all quarks should be restricted. This restriction is for avoiding tree-level FCNC. Therefore, there are generally two possibilities for the two Higgs doublets (H_1 and H_2) for coupling to the fermions (leptons and quarks). In the first possibility, which is usually called Model I, one of the doublets (H_1) couples to all the bosons and the other one (H_2) couples to all the quarks, as in the SM. In this scenario the Yukawa couplings between the charged Higgs boson and the top quark is given by [16]

$$L_I = \frac{g_W}{2\sqrt{2}m_W} V_{tb} \cot\beta \{H^+ \bar{t}[m_t(1-\gamma_5) - m_b(1+\gamma_5)]b\} + \text{H.c.}, \quad (1)$$

where V_{tb} is the CKM matrix element and g_W is the weak-coupling factor.

In the second approach, named Model II, the doublet H_2 couples to the right chiral up-type quarks and the doublet H_1 couples to the right chiral down-type ones. In this model, the interaction Lagrangian reads

$$L_{II} = \frac{g_W}{2\sqrt{2}m_W} V_{tb} \{H^+ \bar{t}[m_t \cot\beta(1-\gamma_5) + m_b \tan\beta(1+\gamma_5)]b\} + \text{H.c.} \quad (2)$$

At the Born-level approximation, the amplitude for the process $H^+ \to t\bar{b}$ is parametrized as $M_0 = v_b(a + b\gamma_5)\bar{u}_t$. In the rest frame of the charged Higgs boson, the tree-level decay width is given by

$$\tilde{\Gamma}_0 = \frac{N_c m_H}{8\pi} \lambda^{\frac{1}{2}}(1, R, y)[2(a^2+b^2)(S-R) - 2(a^2-b^2)\sqrt{Ry}], \quad (3)$$

where, $N_c = 3$ is a color factor and $\lambda(x,y,z) = (x-y-z)^2 - 4yz$ is the Källén function. In the above equation, we defined: $R = (m_b/m_{H^\pm})^2$, $y = (m_t/m_{H^\pm})^2$ and $S = (1 + R - y)/2$, for simplicity. This tree-level decay width is in complete agreement with the result presented in Ref. [17] and in the limit of vanishing bottom quark mass it was discussed in our previous work [15].

Considering the Born-level amplitude and the interaction Lagrangian (1) and (2) for the coupling factors in Model I, one has

$$a^2+b^2=\sqrt{2}|V_{tb}|^2G_F(m_t^2+m_b^2)\cot^2\beta,$$
$$a^2-b^2=-2\sqrt{2}|V_{tb}|^2G_F(m_bm_t)\cot^2\beta, \quad (4)$$

so the same in Model II read as

$$a^2+b^2=\sqrt{2}|V_{tb}|^2G_F(m_t^2\cot^2\beta+m_b^2\tan^2\beta),$$
$$a^2-b^2=2\sqrt{2}|V_{tb}|^2G_F(m_bm_t). \quad (5)$$

In the following, the technical detail of our calculation for the $\mathcal{O}(\alpha_s)$ QCD radiative corrections to the tree-level decay rate of $H^+\to\bar{b}t$ is explained using dimensional regularization approach to regularize all divergences. For this calculation, we apply fixed-flavor-number scheme (FFNs) where $m_b\neq 0$ is considered.

B. Virtual radiative corrections

Generally, the virtual radiative corrections to the tbH^+ vertex consists of both ultraviolet (UV) and infrared (IR) divergences. These UV and IR singularities arise from the hard and soft virtual gluon radiations, respectively. There are different schemes for the renormalization of physical quantities. In this work we adopt the on shell mass-renormalization approach and to regularize all singularities we apply the dimensional regularization scheme in which $D=4-2\epsilon$ is adopted for the dimension of spacetime. Then, all singularities appear as $\epsilon_{\rm UV}$ or $\epsilon_{\rm IR}$.

First, for simplify, we define our kinematic variables as

$$S=\frac{1}{2}(1+R-y),$$
$$\beta=\frac{\sqrt{R}}{S},$$
$$Q=S\sqrt{1-\beta^2},$$
$$\eta=\frac{S-R}{\sqrt{Ry}},$$
$$x_s=\frac{Q+R-S}{\sqrt{Ry}}, \quad (6)$$

where, as before, the scaled masses $y=m_t^2/m_{H^\pm}^2$ and $R=m_b^2/m_{H^\pm}^2$ are defined. Considering these notations the Born-level decay width (3) is simplified as

$$\tilde{\Gamma}_0=\frac{N_cQm_{H^\pm}}{2\pi}[(a^2+b^2)(S-R)-(a^2-b^2)\sqrt{Ry}]. \quad (7)$$

To determine the energy spectrum of B-mesons produced in the decay mode $H^+\to\bar{b}t(+g)\to B+X$ we need to have the quantities $d\tilde{\Gamma}_i/dx_i(i=b,g)$ where

$$x_i=\frac{E_i}{E_b^{\max}}=\frac{E_i}{Sm_{H^\pm}}. \quad (8)$$

Here, x_i stands for the scaled energy of partons (b-quark or gluon) so that x_b ranges as $\beta\le x_b\le 1$.

The contribution of virtual gluon radiation into the differential decay width $d\tilde{\Gamma}_b/dx_b$ reads

$$\frac{d\tilde{\Gamma}_b^{\rm vir}}{dx_b}=\frac{Q}{8\pi m_{H^\pm}}\overline{|M^{\rm vir}|^2}\delta(1-x_b). \quad (9)$$

Here, $\overline{|M^{\rm vir}|^2}=N_c\sum_{\rm Spin}(M_0^\dagger M_{\rm loop}+M_{\rm loop}^\dagger M_0)$ where M_0 is the amplitude at the Born level. In Fig. 1(b), the Feynman diagrams contributing to the virtual corrections are shown. The corresponding renormalized amplitude is written as

$$M_{\rm loop}=v_b(\Lambda_{ct}+\Lambda_l)\bar{u}_t, \quad (10)$$

where Λ_l arises from the one-loop vertex correction and Λ_{ct} includes a combination of wave function renormalization and vertex counterterm. The latter is expressed as [18–21]

$$\Lambda_{ct}=(a+b)\left(\frac{\delta Z_b}{2}+\frac{\delta Z_t}{2}-\frac{\delta m_t}{m_t}\right)\frac{1+\gamma_5}{2}+(a-b)\left(\frac{\delta Z_b}{2}+\frac{\delta Z_t}{2}-\frac{\delta m_b}{m_b}\right)\frac{1-\gamma_5}{2}, \quad (11)$$

where, the wave function and the mass renormalization constants of top and bottom quarks are given by

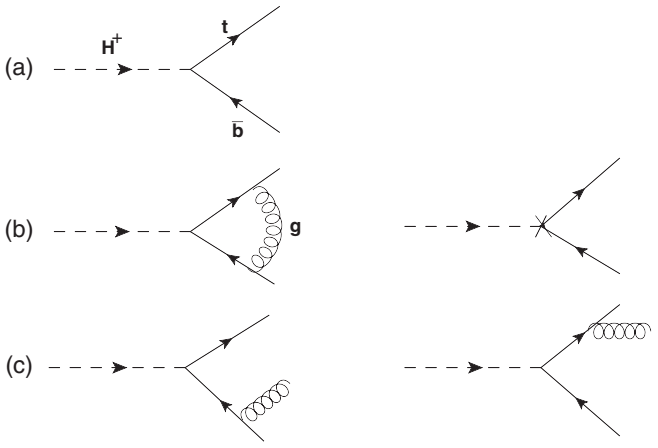

FIG. 1. NLO Feynman diagrams for heavy charged Higgs decay: (a) Lowest-order contribution; (b) vertex correction and combination of wave function renormalization and vertex counterterm; (c) final-state radiation.

$$\frac{\delta m_q}{m_q}=\frac{\alpha_s(\mu_R)}{4\pi}C_F\left(\frac{3}{\epsilon_{\rm UV}}-3\gamma_E+3\ln\frac{4\pi\mu_F^2}{m_q^2}+4\right),$$
$$\delta Z_q=-\frac{\alpha_s(\mu_R)}{4\pi}C_F\left(\frac{1}{\epsilon_{\rm UV}}+\frac{2}{\epsilon_{\rm IR}}-3\gamma_E+3\ln\frac{4\pi\mu_F^2}{m_q^2}+4\right), \quad (12)$$

where, $\gamma_E=0.577216\cdots$ is the Euler constant, $\alpha_s(\mu)$ is the strong coupling constant and $C_F=(N_c^2-1)/(2N_c)=4/3$ for $N_c=3$ quark colors. Moreover, μ_F and μ_R are the factorization and renormalization scales, respectively, which are arbitrarily set as $\mu_R=\mu_F=m_{H^\pm}$.

In addition, the real part of vertex correction reads

$$\Lambda_l=N_c\frac{\alpha_s m_{H^\pm}^2}{\pi}C_F[(a^2-b^2)\sqrt{Ry}G_+ +(a^2+b^2)G_-], \quad (13)$$

where

$$G_+ = 4m_{H^\pm}^2(S-R)C_0(m_b^2,m_t^2,m_{H^\pm}^2,m_b^2,0,m_t^2) - B_0(m_b^2,0,m_b^2)-2B_0(m_{H^\pm}^2,m_b^2,m_t^2) - B_0(m_t^2,0,m_t^2)+2,$$
$$G_- = -4m_{H^\pm}^2(R-S)^2C_0(m_b^2,m_t^2,m_{H^\pm}^2,m_b^2,0,m_t^2) + (1-y)B_0(m_b^2,0,m_b^2)-(R+y)B_0(m_{H^\pm}^2,m_b^2,m_t^2) + (1-R)B_0(m_t^2,0,m_t^2)+2(R-S). \quad (14)$$

Here, the functions B_0 and C_0 are the Passarino-Veltman two-point and three-point integrals, see Ref. [22]. After summing up all contributions arising from virtual corrections the UV singularities are canceled but the IR singularities are remaining which are labeled by ϵ from now on. Finally, the virtual differential decay rate reads

$$\frac{d\tilde{\Gamma}_b^{\rm vir}}{dx_b}=\tilde{\Gamma}_0\frac{\alpha_s(\mu_R)}{2\pi}C_F\delta(1-x_b)\Bigg\{-2+(1-2S)\ln\frac{R}{y} + \frac{1}{a^2-b^2-(a^2+b^2)\eta}\left(3ab\eta\ln\frac{R}{y}+\frac{2Q\ln x_s}{R-S}[(a^2+b^2)\eta(R+y)-2(a^2-b^2)(R-S)]\right) - 2\left[1-\frac{R-S}{Q}\ln x_s\right]\left(\ln\frac{4\pi\mu_F^2}{m_t m_b}-\gamma_E+\frac{1}{\epsilon}\right) + \frac{S-R}{Q}\left[2Li_2\left(1-\frac{m_b}{m_t}x_s\right)+2Li_2\left(1-\frac{m_t}{m_b}x_s\right)-\frac{\pi^2}{3}-\ln^2 x_s+\frac{1}{4}\ln^2\frac{R}{y}+4\ln x_s\ln(1-x_s^2)+2Li_2(x_s^2)\right]\Bigg\}, \quad (15)$$

where, $Li_2(x)=-\int_0^x(dt/t)\ln(1-t)$ is the Spence function and in the Model I one has

$$ab=\frac{G_F}{\sqrt{2}}|V_{tb}|^2(m_t^2-m_b^2)\cot^2\beta, \quad (16)$$

and in Model II, it reads

$$ab=\frac{G_F}{\sqrt{2}}|V_{tb}|^2(m_t^2\cot^2\beta-m_b^2\tan^2\beta). \quad (17)$$

C. Real gluon-radiative corrections

Real gluon radiative corrections are necessary to remove all remaining IR singularities. Considering the two Feynman diagrams shown in Fig. 1(c), the $\mathcal{O}(\alpha_s)$ real gluon emission amplitude reads

$$M^{\rm real}=g_s T^a v(p_b,s_b)\left\{-\frac{m_t+\not{p}_t+\not{p}_g}{2p_t\cdot p_g}+\frac{\not{p}_b+\not{p}_g-m_b}{2p_b\cdot p_g}\right\} \times\gamma^\mu(a\mathbf{1}+b\gamma_5)\bar{u}(p_t,s_t)\epsilon_\mu^\star(p_g,r), \quad (18)$$

where, the generators T^a are related to the Gell-Mann matrices and $\epsilon(p_g,r)$ shows the polarization vector of emitted real gluon with the spin r and four-momentum p_g. Note that, in the massive scheme the IR divergences arise from the soft real gluon emissions while when the b-quark mass is set to zero (massless scheme), the collinear singularities appear too (see our previous work [15]).

According to the dimensional regularization scheme the differential decay rate of process $H^+\to t\bar{b}g$ is given by

$$d\tilde{\Gamma}^{\rm real}=\frac{\mu_F^{2(4-D)}}{2m_{H^\pm}}|M^{\rm real}|^2 dPS(p_t,p_b,p_g,p_{H^+}), \quad (19)$$

where, the phase space element dPS is expressed as

$$\frac{d^{D-1}\vec{p}_b}{2E_b}\frac{d^{D-1}\vec{p}_t}{2E_t}\frac{d^{D-1}\vec{p}_g}{2E_g}(2\pi)^{3-2D}\delta^D\left(p_H-\sum_{g,b,t}p_f\right). \quad (20)$$

To compute the real differential decay rate $d\tilde{\Gamma}_b^{\rm real}/dx_b$ one should fix the b-quark momentum in Eq. (19) and integrates over the energy of gluon x_g which ranges as

$$\frac{(1-x_b)(1-Sx_b-H)}{1+R-2Sx_b}\le x_g\le\frac{(1-x_b)(1-Sx_b+H)}{1+R-2Sx_b}, \quad (21)$$

where $H = S\sqrt{x_b^2 - \beta^2}$. When integrating over the phase space of the process, terms of the form $(1-x_b)^{-1-2\epsilon}$ will appear in the rate $d\tilde{\Gamma}_b^{\text{real}}/dx_b$ which are due to the radiation of soft gluon. Therefore, the following prescription introduced in Ref. [23] is applied

$$\frac{(x_b-\beta)^{2\epsilon}}{(1-x_b)^{1+2\epsilon}} = -\frac{1}{2\epsilon}\delta(1-x_b) + \frac{1}{(1-x_b)_+} + \mathcal{O}(\epsilon), \quad (22)$$

where the plus description of a function is defined as $\int_0^1 (f(x))_+ h(x)dx = \int_0^1 f(x)[h(x)-h(1)]dx$.

D. Parton-level results of $d\tilde{\Gamma}_i/dx_i$ in FFN scheme

Ignoring the details, by summation of the tree-level, the virtual and real gluon radiative contributions one obtains the following analytical result for the differential decay rate of $H^+ \to t\bar{b}$,

$$\begin{aligned}
\frac{1}{\tilde{\Gamma}_0}\frac{d\tilde{\Gamma}_b}{dx_b} &= \delta(1-x_b) + \frac{C_F\alpha_s(\mu_R)}{2\pi}\left\{\delta(1-x_b)\left[(y-R)\ln R + 2(1+S)\ln y + \frac{S-R}{2Q}\ln^2\frac{R}{y} - \ln(8Q^2)\right.\right. \\
&+ \frac{1}{\eta(a^2+b^2)-(a^2-b^2)}\left(-3ab\eta\ln\frac{R}{y} + 2Q\ln x_s\left[2(a^2-b^2) + (a^2+b^2)\frac{R+y}{\sqrt{Ry}}\right]\right) \\
&+ \frac{2(S-R)}{Q}\left[Li_2\left(1-\frac{m_b}{m_t}x_s\right) + Li_2\left(1-\frac{m_t}{m_b}x_s\right) - Li_2(1-x_s^2) - \ln x_s - \frac{1}{2}\ln^2\frac{m_b x_s}{m_t}\right] + 2\left(1+\frac{S-R}{Q}\ln x_s\right)\ln\frac{1+\beta}{1-\beta} \\
&+ \frac{a^2+b^2}{a^2-b^2-\eta(a^2+b^2)}\left[4\frac{a^2-b^2}{a^2+b^2}\times\frac{Q-S\sqrt{x_b^2-\beta^2}}{Q(1-x_b)} - \frac{4\eta}{1-x_b} + \frac{2S\eta\sqrt{x_b^2-\beta^2}}{Q(R-S)(1+R-2Sx_b)^2}\left(S^3(1-x_b)(10-3x_b)\right.\right. \\
&\left.\left.\left. + \frac{2y^2(y-1)}{1-x_b} - S^2x_b(9y-7) + S^2(17y-7) - \frac{2Sy}{1-x_b}[4-5y+4x_b(y-1)]\right)\right] + \frac{2}{Q(a^2-b^2-(a^2+b^2)\eta)} \\
&\left.\times\ln\frac{R-S(x_b-\sqrt{x_b^2-\beta^2})}{R-S(x_b+\sqrt{x_b^2-\beta^2})}\left[\frac{R-Sx_b}{(1-x_b)_+}(a^2-b^2) + \frac{a^2+b^2}{\sqrt{Ry}}\left[\frac{S^2(1+x_b)}{2} + \frac{R^2+S^2x_b^2-RS(1+x_b)}{(1-x_b)_+}\right]\right]\right\}. \quad (23)
\end{aligned}$$

Since, bottom-flavored hadrons can also be produced from the fragmentation of real gluons emitted at NLO then to have the most accurate energy spectrum of B-mesons we have to consider the contribution of gluon fragmentation as well. Then we also need the differential decay rate $d\tilde{\Gamma}_g/dx_g$ in the FFN scheme where $x_g = E_g/(Sm_{H^\pm})$, as in Eq. (8), is the scaled-energy fraction of the real gluon emitted. Note that, the contribution of gluon splitting is significant at the low energy of observed B-hadrons and decreases the size of decay rate at the threshold (see Refs. [24–26]). In order to calculate the $d\tilde{\Gamma}_g/dx_g$, in Eq. (19) we integrate over the momentum of bottom quark by fixing the momentum of gluon in the phase space. By ignoring more details, this contribution reads

$$\begin{aligned}
\frac{1}{\tilde{\Gamma}_0}\frac{d\tilde{\Gamma}_g}{dx_g} &= \frac{C_F\alpha_s(\mu_R)}{2\pi Qx_g}\left\{-4S(1-x_g)F + \frac{1}{(R-S)(b^2-a^2+\eta(a^2+b^2))}[2(a^2-b^2)(S-R)(R-S+Sx_g)\right. \\
&+ \eta(a^2+b^2)(2R^2+2RS(x_g-2)+S^2(x_g^2-2x_g+2))] \\
&\left.\times\left(\ln\frac{1-F}{1+F} - \ln\frac{x_g-Sx_g[1+x_g+(x_g-1)F]}{x_g-Sx_g[1+x_g-(x_g-1)F]}\right)\right\}, \quad (24)
\end{aligned}$$

where $F = \sqrt{1-\beta^2(1-2Sx_g)/(1-x_g)^2}$.

III. GM-VFN SCHEME

Since, the proposed channel to search for heavy charged Higgs bosons is to study the energy spectrum of B-mesons inclusively produced in the decay mode $H^+ \to t\bar{b}(\to B + \text{jets})$ then we need to calculate the partial decay width of this process differential in x_B, i.e., $d\Gamma/dx_B$. Here, $x_B = E_B/(Sm_{H^\pm})$ is the scaled energy fraction of the B-meson, as in Eq. (8). In the charged Higgs rest frame, the energy of B-meson is $E_B = p_H \cdot p_B/m_{H^\pm}$ so it ranges as $m_B \le E_B \le [m_{H^\pm}^2 + m_B^2 - m_t^2]/(2m_{H^\pm})$. In the case of gluon splitting it ranges as $m_B \le E_B \le [m_{H^\pm}^2 + m_B^2 - (m_b+m_t)^2]/(2m_{H^\pm})$.

The key tool to calculated the energy distribution of B-meson is the factorization theorem of QCD [27]. According to that, the B-meson energy spectrum is obtained by the convolution of parton-level spectrum ($H^+ \to \bar{b}t + g$) with the nonperturbative fragmentation function $D_i^B(z, \mu_F)$, i.e.,

$$\frac{d\Gamma}{dx_B} = \sum_{i=b,g} \int_{x_i^{\min}}^{x_i^{\max}} \frac{dx_i}{x_i} \frac{d\Gamma_i^{\mathrm{GM}}}{dx_i}(\mu_R, \mu_F) D_i^B\left(\frac{x_B}{x_i}, \mu_F\right), \tag{25}$$

where, $d\Gamma_i^{\mathrm{GM}}/dx_i$ is the differential decay width of the process $H^+ \to \bar{b}t$ in the GM-VFN scheme. In the following, evaluation of the quantity $d\Gamma_i^{\mathrm{GM}}(\mu_R, \mu_F)/dx_i$ is discussed in detail.

In our previous work [15], we computed the quantity $d\hat{\Gamma}_i^{\mathrm{NLO}}(H^+ \to \bar{b}t)/dx_i (i = b, g)$ in the massless or zero-mass variable-flavor-number scheme where $m_b = 0$ was adopted from the beginning. Our result for $\hat{\Gamma}(H^+ \to \bar{b}t)$, after integrating $d\hat{\Gamma}(H^+ \to \bar{b}t)/dx_b$ over $0 \le x_b \le 1$, was found to be in complete agreement with the one presented in Ref. [17]. However, the massless scheme makes the calculations so simple but leads to waste all information on the m_b-dependence of $d\hat{\Gamma}_i/dx_i$. In the massive scheme, $m_b \neq 0$ only sets the initial scale $\mu_F^{\mathrm{ini}} = \mathcal{O}(m_b)$ of Dokshitzer-Gribov-Lipatov-Altarelli-Parisi (DGLAP) evolution equations [28].

In the previous section we employed the FFN scheme, which contains of full m_b dependence, and computed the massive results which are presented for the first time. In the FFN scheme, the large logarithmic singularities of the form $\alpha_s \ln R = \alpha_s \ln(m_b^2/m_{H^\pm}^2)$ spoil the convergence of perturbative expansion when $m_b \to 0$ [see Eq. (23)]. The GM-VFN scheme is an elaborate approach which is designed for resuming the large logarithmic terms in m_b. This aim is achieved by introducing suitable subtraction terms in the NLO FFN expressions of $d\tilde{\Gamma}_i/dx_i$. In conclusion, the NLO results at the massless scheme are exactly recovered in the limit $m_b \to 0$. Following Refs. [29,30], the subtraction terms are constructed as

$$\frac{1}{\Gamma_0}\frac{d\Gamma_i^{\mathrm{Sub}}}{dx_i} = \lim_{m_b \to 0} \frac{1}{\tilde{\Gamma}_0}\frac{d\tilde{\Gamma}_i^{\mathrm{FFN}}}{dx_i} - \frac{1}{\hat{\Gamma}_0}\frac{d\hat{\Gamma}_i^{\mathrm{ZM}}}{dx_i}. \tag{26}$$

Therefore, by subtracting the subtraction terms from the FFN results the GM-VFN differential decay rates are obtained as

$$\frac{1}{\Gamma_0}\frac{d\Gamma_i^{\mathrm{GM}}}{dx_i} = \frac{1}{\tilde{\Gamma}_0}\frac{d\tilde{\Gamma}_i^{\mathrm{FFN}}}{dx_i} - \frac{1}{\Gamma_0}\frac{d\Gamma_i^{\mathrm{Sub}}}{dx_i}. \tag{27}$$

By taking the limit $R \to 0 \equiv m_b \to 0$ in Eqs. (23) and (24), we obtain the following subtraction terms

$$\frac{1}{\Gamma_0}\frac{d\Gamma_b^{\mathrm{Sub}}}{dx_b} = -\frac{\alpha_s(\mu_R)}{2\pi} C_F \times \left\{ \frac{1+x_b^2}{1-x_b} [\ln R + 2\ln(1-x_b) + 1] \right\}_+, \tag{28}$$

$$\frac{1}{\Gamma_0}\frac{d\Gamma_g^{\mathrm{Sub}}}{dx_g} = -\frac{\alpha_s(\mu_R)}{2\pi} C_F \left\{ \frac{1+(1-x_g)^2}{x_g} \times \left[\ln R - \ln \frac{4S(1-x_g)}{x_g\sqrt{1-2Sx_g}} \right] + \frac{(2-x_g)^2}{2x_g} \right\}. \tag{29}$$

The subtraction terms are universal [27,31] and Eq. (28) coincides with the perturbative FF of the transition $b \to b$ [24,31]. It should be noted that, the correctness of our calculations could be confirmed by two facts; all singularities of parton level at NLO are being removed and the universal subtraction term (28) is extracted. Although, in our previous work [15] we have shown that our analytical result for $d\hat{\Gamma}^{\mathrm{NLO}}(H^+ \to \bar{b}t)/dx_b$ at the massless scheme after integrating $d\hat{\Gamma}(H^+ \to \bar{b}t)/dx_b$ over $0 \le x_b \le 1$ was in complete agreement with the one presented in Ref. [17].

IV. NUMERICAL ANALYSIS

In this section we present our phenomenological predictions for the energy spectrum of B-mesons inclusively produced in the decay of heavy charged Higgs bosons. In the context of 2HDMs, various searches for the signature $H^+ \to t\bar{b}$ have been done by the CERN ATLAS and CMS Collaborations in proton-proton collisions at the center-of-mass energies of 8 TeV and 13 TeV [11–13]. As a review, Fig. 7 in Ref. [12] shows the excluded parameter space in the MSSM scenarios where the excluded maximum value of $\tan\beta$ is 0.88 for $0.20 < m_{H^\pm} < 0.55$ TeV. The same searches have been carried out by ATLAS Collaboration at $\sqrt{s} = 13$ TeV [32] which have excluded $m_{H^\pm} \approx 300$–900 GeV for a very low $\tan\beta$ region, i.e., $\tan\beta \approx 0.5$–1.7. Also, for large values of $\tan\beta > 44(60)$, the value $m_{H^\pm} \approx 300(366)$ GeV is excluded. Nevertheless, a definitive search over the $m_{H^\pm} - \tan\beta$ parameter space is a program that still has to be carried out by the LHC experiments and future colliders.

Throughout this work, we restrict ourselves to the allowed regions of the $m_{H^\pm} - \tan\beta$ parameter space evaluated by the CMS experiments, see Fig. 7 in Ref. [12]. For the input parameters, we adopt the values $G_F = 1.16637 \times 10^{-5}\,\mathrm{GeV}^{-2}$, $m_t = 172.98\,\mathrm{GeV}$, $m_b = 4.90$ GeV, $m_B = 5.279$ GeV, and $|V_{tb}| = 0.999152$ [33]. Taking $m_{H^\pm} = 500$ GeV and $\tan\beta = 6$, for the Born-level decay rates in the massless and massive schemes one has

$$\tilde{\Gamma}_0^{\rm GM} = 0.635 \quad (\textbf{Model I}),$$
$$\tilde{\Gamma}_0^{\rm GM} = 1.283 \quad (\textbf{Model II}),$$
$$\hat{\Gamma}_0^{\rm ZM} = 0.634 \quad (\textbf{both models}). \tag{30}$$

Note that, in spite of the fact that $m_b \ll m_t$, in Model II the contribution $m_b^2 \tan^2\beta$ (the left-chiral coupling term) in the combination $a^2 + b^2$ (5) can not always be ignored in comparison to the term $m_t^2 \cot^2\beta$ (the right-chiral coupling term) when $\tan\beta$ is large. While, in Model I (4) the term m_b^2 can always be ignored in comparison to the term m_t^2. This is why one has $\tilde{\Gamma}_0^{\rm GM,I} \approx \tilde{\Gamma}_0^{\rm ZM}$ in Eq. (30) while $\tilde{\Gamma}_0^{\rm GM,II} \approx 2\tilde{\Gamma}_0^{\rm ZM}$.

In next step, to predict the energy spectrum of B-mesons we back to the relation (25). Considering this equation, we also need the nonperturbative fragmentation functions $D_i^B (i = b, g)$ describing the hadronization processes $(b, g) \to B$. For these transitions, we use the realistic nonperturbative fragmentation functions of B-meson determined at NLO through a global fit to electron-positron annihilation data presented by ALEPH [34] and OPAL [35] at CERN LEP1 and by SLD [36] at SLAC SLC. In literature, different phenomenological models have been proposed to describe the hadronization mechanism. Among them, the power model $D_b(z, \mu_F^{\rm ini}) = N z^\alpha (1-z)^\beta$ is well established. In Ref. [37], we have extracted the free parameters of this model for the fragmentations of all light and heavy partons into B-meson at the initial scale $\mu_F^{\rm ini} = 4.5$ GeV. Our fit for the $b \to B$ splitting yielded $N = 2575.014$, $\alpha = 15.424$, and $\beta = 2.394$. The fragmentation function of gluon is generally assumed to be zero at the initial scale and is generated via the DGLAP evolution equations [28]. In Refs. [21,38], we have showed that the contribution of $g \to B$ transition in $d\Gamma/dx_B$ is negative and considerable only in the low-x_B region. For larger values of x_B the result is practically governed by the $b \to B$ transition.

In Figs. 2 and 4 our predictions for the energy spectrum of B-mesons are presented by plotting $d\Gamma/dx_B$ versus x_B in Model I and II, respectively. For this study we fixed $\tan\beta = 2$ and the different values of heavy charged Higgs masses are considered, i.e., $m_{H^\pm} = 200$, 300, and 400 GeV. The B-meson mass is responsible for the thresholds at $x_B = 0.19$ (for $m_{H^\pm} = 200$ GeV), $x_B = 0.07$ (for $m_{H^+} = 300$ GeV), and $x_B = 0.056$ (for $m_{H^\pm} = 400$ GeV). As is seen, by increasing the Higgs boson mass the

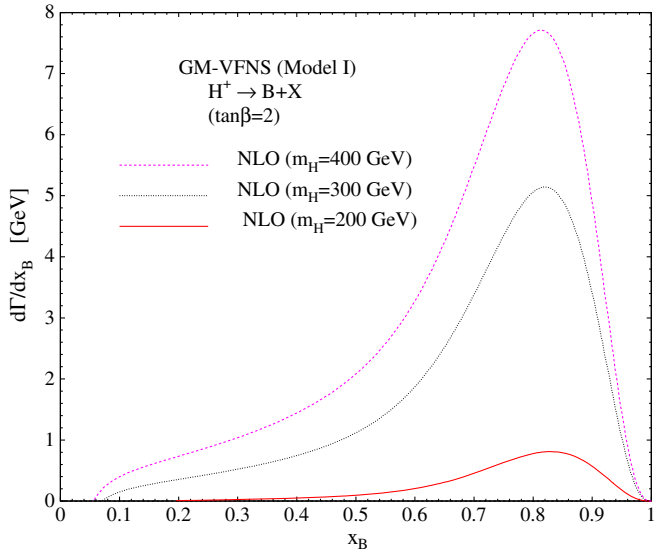

FIG. 2. The x_B spectrum in heavy charged Higgs decay $(H^+ \to BX)$ in the massive scheme (or GM-VFNs) for Model I, taking $\tan\beta = 2$ and $m_{H^\pm} = 200$, 300, and 400 GeV.

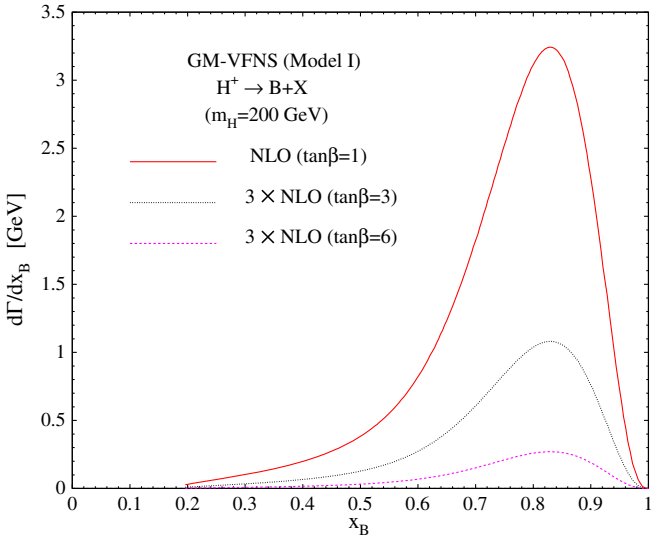

FIG. 3. $d\Gamma(H^+ \to BX)/dx_B$ versus x_B in the GM-VFN scheme for Model I taking $m_{H^\pm} = 200$ GeV and $\tan\beta = 1$, 3, and 6.

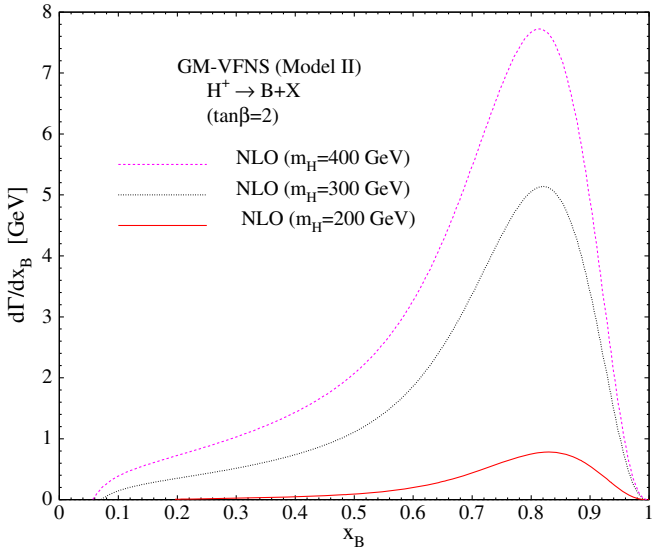

FIG. 4. As in Fig. 2 but for Model II.

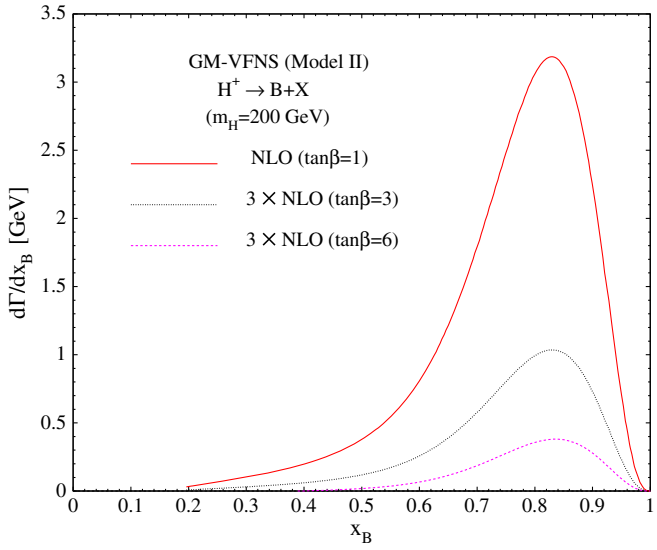

FIG. 5. As in Fig. 3 but for Model II.

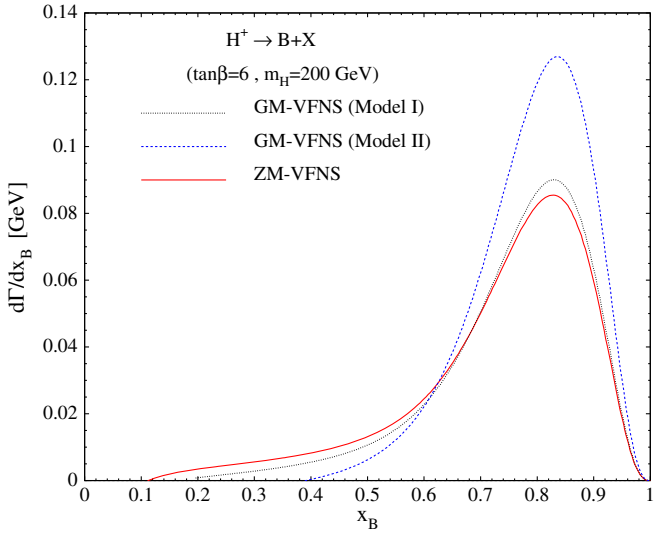

FIG. 7. As in Fig. 6 but for $m_{H^\pm} = 200$ GeV and $\tan\beta = 6$.

size of partial decay width increases. In Figs. 3 and 5, the same studies have been done by fixing the Higgs mass ($m_{H^\pm} = 200$ GeV) and taking different values of $\tan\beta = 1$, 3, and 6. It can be seen that when $\tan\beta$ increases the size of decay rate decreases and the peak position is shifted towards higher values of x_B.

In Figs. 6 and 7, the energy spectrum of B-meson is compared in the GM-VFN ($m_b \neq 0$) and ZM-VFN ($m_b = 0$) schemes, using $\tan\beta = 1$, 6, and $m_{H^\pm} = 200$ GeV. As it is observed from Fig. 6, the results of both models in the GM-VFN scheme and the one in the ZM-VFN scheme are approximately the same. But Fig. 7 (with $\tan\beta = 6$) shows that the energy spectrum of B-meson in the ZM- and GM-VFN schemes (Model I) are approximately the same while the one in GM-VFNs for Model II is completely different. In Figs. 8 and 9 we have studied the x_B spectrum in the massless and massive schemes using $\tan\beta = 2$, 6, and $m_{H^\pm} = 500$ GeV. It is seen that for heavier Higgses the results obtained in the massive scheme are completely different with the one obtained in the ZM-VFN scheme. In other words, the massless approximation does not always work well and most reliable predictions are made at NLO in the GM-VFN scheme. Generally, the results for energy spectrum of B-meson in the 2HDM are extremely model dependent.

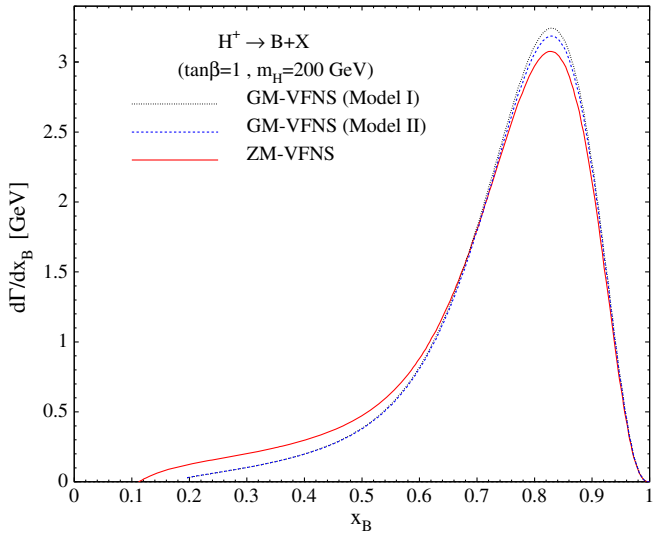

FIG. 6. The x_B spectrum in the decay mode $H^+ \to BX$ at NLO. The GM-VFNs results in the two models (I and II) are compared to the one in the ZM-VFN scheme. Here, we fixed $m_{H^\pm} = 200$ GeV and $\tan\beta = 1$.

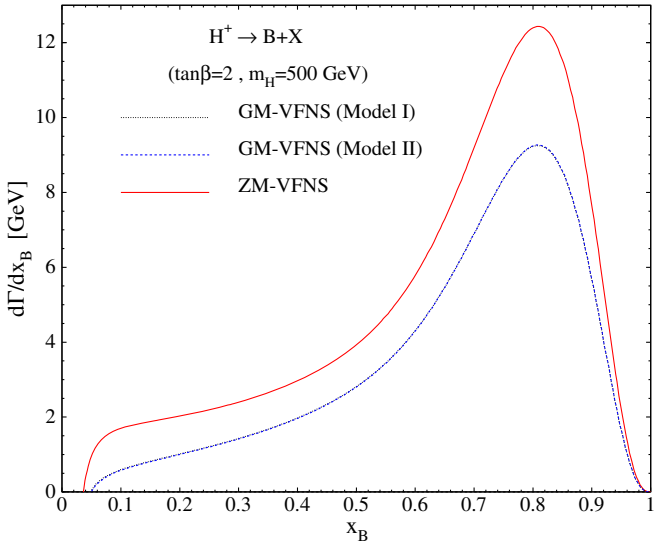

FIG. 8. As in Figs. 6 and 7, but taking $m_{H^\pm} = 500$ GeV and $\tan\beta = 2$.

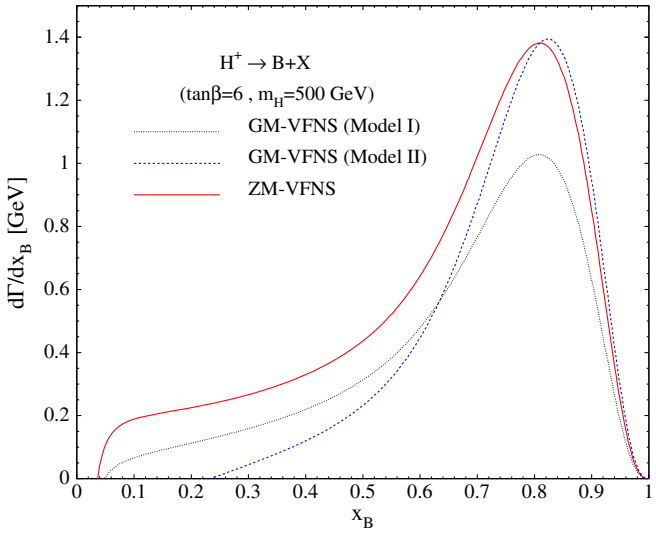

FIG. 9. As in Figs. 8, but for $m_{H^\pm} = 500$ GeV and $\tan\beta = 6$.

V. CONCLUSIONS

Despite of all successes of the ordinary SM it can not be a theory of everything since there are still many unsolved questions that this model dose not have definite replies for them. To solve the remaining problems many theories have been suggested so among them the most important ones are those based on the supersymmetry. These theories often include an extended Higgs sector which lead to appear new elementary particles. As an example, in the theory of minimal supersymmetry five Higgs particles are created; three neutral bosons and two charged bosons $H^\pm$. The discovery of each of them would be an immediate evidence of new physics beyond the standard model. By this explanation, searches for light or heavy charged Higgs bosons (lighter or heavier than the top quark) are strongly motivated and these have been main goals of many high energy colliders in recent years. However, no explicit evidence has been yet found. With respect to the searches done by the CMS and ATLAS Collaborations a large region in the MSSM $m_{H^\pm} - \tan\beta$ parameter space has been excluded. Then, it seems that most efforts have to concentrate on probing heavy charged Higgs bosons. These scalar heavy bosons are anticipated to decay predominantly either to a tau or a top quark. Although, the second decay mode, i.e., $H^+ \to t\bar{b}$, suffers from a large multijet background but it dominates in the region of heavy masses.

In our previous work [15], through the 2HDM we studied the dominant decay channel $H^+ \to t\bar{b}(+g)$ followed by the hadronization process $(b, g) \to B$. For this study we evaluated the distribution in the scaled energy (x_B) of B-mesons which would be of particular interest at the LHC and future colliders to search for charged Higgs bosons. To this aim we worked in the ZM-VFN scheme where the b-quark mass is ignored from the beginning and showed that results are the same in both Type-I and Type-II scenarios (Models I and II). Although this scheme makes calculations so simple but it leads to spoil all information on the m_b dependence of B-hadron spectrum. In the present work, we studied the same decay channel but in the GM-VFN scheme in which the b-quark mass is preserved from the beginning. We first computed an analytic expression for the NLO radiative corrections to the differential decay width of charged Higgs bosons at the parton level, i.e., $d\tilde{\Gamma}_i^{\rm NLO}(H^+ \to \bar{b}t)/dx_i (i = b, g)$. In the following, using the nonperturbative fragmentation functions of $(b, g) \to B$ the x_B spectrum is predicted. Our results showed that for lighter Higgses ($m_{H^\pm} \approx 200$ GeV) and small values of $\tan\beta$ the massive results for two models are the same and coincide with the one in the massless scheme. But in the general case the massive results for two models and the one evaluated in the massless scheme are completely different, specifically, when $m_{H^\pm}$ is large.

Our analysis is expected to make a contribution to the LHC searches for charged Higgses. Moreover, a comparison between future measurements of x_B spectrum and the presented predictions will be important for our understanding of the Higgs coupling in 2HDM and new physics beyond the SM. Our analysis can be extended to the production of other hadrons such as pions, kaons, and protons, etc., for which one needs the corresponding fragmentation functions $(b, g) \to \pi/K/P/D^+$ presented in Refs. [39–44].

[1] T. Aaltonen *et al.* (CDF Collaboration), High-precision measurement of the W boson mass with the CDF II detector, Science **376**, 170 (2022).
[2] T. D. Lee, A theory of spontaneous T violation, Phys. Rev. D **8**, 1226 (1973).
[3] A. Djouadi, The anatomy of electro-weak symmetry breaking. II. The Higgs bosons in the minimal supersymmetric model, Phys. Rep. **459**, 1 (2008).
[4] J. F. Gunion and H. E. Haber, Higgs bosons in supersymmetric models. 1, Nucl. Phys. **B272**, 1 (1986); **402**, 567 (1993).
[5] CMS Collaboration (CMS Collaboration), Search for charged Higgs bosons with the H+ to tau nu decay channel in the fully hadronic final state at sqrt s = 8 TeV, CERN Report No. CMS-PAS-HIG-14-020.
[6] The ATLAS Collaboration (ATLAS Collaboration), Search for charged Higgs bosons in the τ + jets final state with pp

collision data recorded at $\sqrt{s} = 8$ TeV with the ATLAS experiment, CERN Report No. ATLAS-CONF-2013-090.
[7] A. Pich and P. Tuzon, Yukawa alignment in the two-Higgs-doublet model, Phys. Rev. D **80**, 091702 (2009).
[8] J. Hernandez-Sanchez, S. Moretti, R. Noriega-Papaqui, and A. Rosado, Off-diagonal terms in Yukawa textures of the Type-III 2-Higgs doublet model and light charged Higgs boson phenomenology, J. High Energy Phys. 07 (2013) 044.
[9] A. G. Akeroyd, S. Moretti, and J. Hernandez-Sanchez, Light charged Higgs bosons decaying to charm and bottom quarks in models with two or more Higgs doublets, Phys. Rev. D **85**, 115002 (2012).
[10] ATLAS Collaboration, Search for a light charged Higgs boson in $t \to H^{\wedge} + b$ decays, with $H^{\wedge} + \to cb$, in the lepton + jets final state in proton-proton collisions at $\sqrt{s} =$ 13 TeV with the ATLAS detector, CERN Report No. ATLAS-CONF-2021-037.
[11] G. Aad *et al.* (ATLAS Collaboration), Search for charged Higgs bosons in the $H^{\pm} \to tb$ decay channel in pp collisions at $\sqrt{s} = 8$ TeV using the ATLAS detector, J. High Energy Phys. 03 (**2016**) 127.
[12] A. M. Sirunyan *et al.* (CMS Collaboration), Search for charged Higgs bosons decaying into a top and a bottom quark in the all-jet final state of pp collisions at $\sqrt{s} = 13$ TeV, J. High Energy Phys. 07 (2020) 126.
[13] The ATLAS Collaboration, Search for charged Higgs bosons decaying into a top-quark and a bottom-quark at $\sqrt{s} = 13$ TeV with the ATLAS detector, CERN Report No. ATLAS-CONF-2020-039.
[14] G. Aad *et al.* (ATLAS Collaboration), Search for charged Higgs bosons decaying into a top quark and a bottom quark at $\sqrt{s} = 13$ TeV with the ATLAS detector, J. High Energy Phys. 06 (2021) 145.
[15] S. M. Moosavi Nejad and P. Sartipi Yarahmadi, Probing heavy charged Higgs bosons through bottom flavored hadrons in the $H^+ \to \bar{b}t \to B + X$ channel in 2HDM, Eur. Phys. J. C **81**, 308 (2021).
[16] J. F. Gunion, H. Haber, G. Kane, and S. Dawson, *The Higgs Hunter's Guide* (Addison-Wesley, Reading, MA, 1990), and references therein.
[17] C. S. Li and R. J. Oakes, QCD corrections to the hadronic decay width of a charged Higgs boson, Phys. Rev. D **43**, 855 (1991).
[18] A. Kadeer, J. G. Körner, and M. C. Mauser, A phenomenological study of bottom quark fragmentation in top quark decay, Eur. Phys. J. C **54**, 175 (2008).
[19] A. Czarnecki and S. Davidson, On the QCD corrections to the charged Higgs decay of a heavy quark, Phys. Rev. D **47**, 3063 (1993).
[20] J. Liu and Y. P. Yao, QCD corrections to the charged Higgs boson decay of a heavy top quark, Phys. Rev. D **46**, 5196 (1992).
[21] S. M. Moosavi Nejad, $\mathcal{O}(\alpha_s)$ corrections to the B-hadron energy distribution of the top decay in the minimal supersymmetric standard model considering GM-VFN scheme, Eur. Phys. J. C **72**, 2224 (2012).
[22] S. Dittmaier, Separation of soft and collinear singularities from one loop N point integrals, Nucl. Phys. **B675**, 447 (2003).
[23] G. Corcella and A. D. Mitov, Bottom quark fragmentation in top quark decay, Nucl. Phys. **B623**, 247 (2002).
[24] B. A. Kniehl, G. Kramer, and S. M. M. Nejad, Bottom-flavored hadrons from top-quark decay at next-to-leading order in the general-mass variable-flavor-number scheme, Nucl. Phys. **B862**, 720 (2012).
[25] S. M. Moosavi Nejad and M. Balali, Hadron energy spectrum in polarized top quark decays considering the effects of hadron and bottom quark masses, Eur. Phys. J. C **76**, 173 (2016).
[26] S. M. Moosavi Nejad and M. Balali, Angular analysis of polarized top quark decay into B-mesons in two different helicity systems, Phys. Rev. D **90**, 114017 (2014); Erratum, Phys. Rev. D **93**, 119904 (2016).
[27] J. C. Collins, Finite-mass effects on inclusive B meson hadroproduction, Phys. Rev. D **58**, 094002 (1998).
[28] V. N. Gribov and L. N. Lipatov, Deep inelastic e p scattering in perturbation theory, Yad. Fiz. **15**, 781 (1972) [Sov. J. Nucl. Phys. **15**, 438 (1972)], https://inspirehep.net/literature/73449; G. Altarelli and G. Parisi, Asymptotic freedom in parton language, Nucl. Phys. **B126**, 298 (1977); Yu. L. Dokshitzer, Calculation of the structure functions for deep inelastic scattering and e+ e− annihilation by perturbation theory in quantum chromodynamics, Zh. Eksp. Teor. Fiz. **73**, 1216 (1977) [Sov. Phys. JETP **46**, 641 (1977)], https://inspirehep.net/literature/126153.
[29] B. A. Kniehl, G. Kramer, I. Schienbein, and H. Spiesberger, Inclusive $D^{*\pm}$ production in p anti-p collisions with massive charm quarks, Phys. Rev. D **71**, 014018 (2005).
[30] B. A. Kniehl, G. Kramer, I. Schienbein, and H. Spiesberger, Reconciling Open Charm Production at the Fermilab Tevatron with QCD, Phys. Rev. Lett. **96**, 012001 (2006).
[31] B. Mele and P. Nason, The fragmentation function for heavy quarks in QCD, Nucl. Phys. **B361**, 626 (1991); J. P. Ma, Perturbative prediction for parton fragmentation into heavy hadron, Nucl. Phys. **B506**, 329 (1997); S. Keller and E. Laenen, Next-to-leading order cross-sections for tagged reactions, Phys. Rev. D **59**, 114004 (1999); M. Cacciari and S. Catani, Soft-gluon resummation for the fragmentation of light and heavy quarks at large x, Nucl. Phys. **B617**, 253 (2001); K. Melnikov and A. Mitov, Perturbative heavy quark fragmentation function through $\mathcal{O}(\alpha_s^2)$, Phys. Rev. D **70**, 034027 (2004); A. Mitov, Perturbative heavy quark fragmentation function through $\mathcal{O}(\alpha_s^2)$: Gluon initiated contribution, Phys. Rev. D **71**, 054021 (2005).
[32] The ATLAS Collaboration, Search for charged Higgs bosons in the $H^{\pm} \to tb$ decay channel in pp collisions at $\sqrt{s} = 13$ TeV using the ATLAS detector, CERN Report No. ATLAS-CONF-2016-089.
[33] K. Nakamura *et al.* (Particle Data Group), Review of particle physics, J. Phys. G **37**, 075021 (2010).
[34] A. Heister *et al.* (ALEPH Collaboration), Study of the fragmentation of b quarks into B mesons at the Z peak, Phys. Lett. B **512**, 30 (2001).
[35] G. Abbiendi *et al.* (OPAL Collaboration), Inclusive analysis of the b quark fragmentation function in Z decays at LEP, Eur. Phys. J. C **29**, 463 (2003).

[36] K. Abe *et al.* (SLD Collaboration), Precise Measurement of the b-Quark Fragmentation Function in Z^0 Boson Decays, Phys. Rev. Lett. **84**, 4300 (2000); Measurement of the b-quark fragmentation function in Z^0 decays, Phys. Rev. D **65**, 092006 (2002); **66**, 079905 (2002).

[37] M. Salajegheh, S. M. Moosavi Nejad, H. Khanpour, B. A. Kniehl, and M. Soleymaninia, B-hadron fragmentation functions at next-to-next-to-leading order from a global analysis of e^+e^- annihilation data, Phys. Rev. D **99**, 114001 (2019).

[38] S. M. Moosavi Nejad, B-mesons from top-quark decay in presence of the charged-Higgs boson in the zero-mass variable-flavor-number scheme, Phys. Rev. D **85**, 054010 (2012).

[39] M. Soleymaninia, A. N. Khorramian, S. M. Moosavi Nejad, and F. Arbabifar, Determination of pion and kaon fragmentation functions including spin asymmetries data in a global analysis, Phys. Rev. D **88**, 054019 (2013).

[40] S. M. Moosavi Nejad, M. Soleymaninia, and A. Maktoubian, Proton fragmentation functions considering finite-mass corrections, Eur. Phys. J. A **52**, 316 (2016).

[41] M. Salajegheh, S. M. Moosavi Nejad, and M. Delpasand, Determination of D_s^+ meson fragmentation functions through two different approaches, Phys. Rev. D **100**, 114031 (2019).

[42] M. Salajegheh, S. M. Moosavi Nejad, M. Soleymaninia, H. Khanpour, and S. Atashbar Tehrani, NNLO charmed-meson fragmentation functions and their uncertainties in the presence of meson mass corrections, Eur. Phys. J. C **79**, 999 (2019).

[43] S. M. Moosavi Nejad, NLO QCD corrections to triply heavy baryon fragmentation function considering the effect of nonperturbative dynamics of baryon bound states, Phys. Rev. D **96**, 114021 (2017).

[44] S. M. Moosavi Nejad, The effect of meson wave function on heavy-quark fragmentation function, Eur. Phys. J. A **52**, 127 (2016).